THE ROYAL SOCIETY

The Earth's deep interior: advances in theory and experiment

By Lidunka Vočadlo and David Dobson

Research School of Geological and Geophysical Sciences, Birkbeck College and University College London, Gower Street, London WC1E 6BT, UK
(l.vocadlo@ucl.ac.uk; d.dobson@ucl.ac.uk)

The Earth extends some 6400 km to the centre, where the conditions of pressure (P) and temperature (T) reach over three million times atmospheric pressure and *ca.* 6000 °C. We stand on thin brittle crustal plates moving through geological time over a continuously deforming mantle of slowly convecting hot rock. The mantle extends about halfway through the Earth to a liquid outer core and a solid inner core. Although the mantle and core make up 99% of the Earth by volume and mass, we are only able to sample mantle material directly to a few hundred kilometres, from inclusions in diamonds that are brought up to the surface by volcanic intrusions; the remaining 90% of the Earth is effectively inaccessible. The most direct knowledge we have of the Earth's deep interior comes from the seismic waves generated from earthquakes. A knowledge of material properties coupled with these seismic waves tell us that the mantle is made up of complex silicates and that the core is predominantly made of solid and liquid iron with some alloying elements. However, the detailed structure of the Earth's deep interior is poorly constrained. Major advances toward the understanding of the composition, structure and dynamics of the Earth's deep interior are to be gained only by a combination of experimental and theoretical techniques. It is already clear that many of the large-scale geological processes responsible for the conditions at the surface are driven from the Earth's core. However, there are many questions yet to be answered about the exact nature of the core and mantle, and the interaction between them. For example, we have yet to fully define the major- and minor-element chemistry of the mantle, the convective regime of the mantle, the alloying elements in the core, the nature of the core–mantle boundary and the dynamical processes in the outer core governing the geodynamo. Advances in high-P/T experimental techniques over the last two decades allow laboratory simulation of the physical conditions from the surface of the Earth to the core, shedding light on the physics and chemistry of the Earth's deep interior. High P and T can be maintained for significant periods (minutes to days) in multi-anvil and diamond-anvil presses. Shock experiments produce high T and P in the megabar range for tiny durations (milliseconds), but, in doing so, they shed light on the physics of the solid inner core. The current development of *in situ* high-pressure research such as P- and S-wave interferometry, electrical conductivity and synchrotron-based X-ray techniques will, over the coming decades, allow significant improvements in our understanding of processes in the deep Earth. Even so, with increasing depth, it becomes increasingly difficult to mimic the extreme conditions of P and T precisely. An alternative to laboratory experiments is the use of computer simulations, which

Phil. Trans. R. Soc. Lond. A (1999) **357**, 3335–3357

allow us to test which models best match the seismic evidence and experimental data. In particular, with increasingly powerful supercomputer resources, emphasis is now being placed on the use of *ab initio* quantum-mechanical calculations to simulate materials at the conditions of pressure and temperature to be found in the Earth's deep interior. This approach allows us to predict the properties of candidate mantle silicates with remarkable accuracy when compared with seismic data and the results of laboratory experiments. With these simulation techniques, we are also trying to solve many problems that are out of the reach of experimentation involving simultaneously high P and T, such as the nature of iron and iron alloys under the extreme conditions of the core where iron is squeezed to about half its normal volume, and we will soon be able provide constraints on the temperature profile of the Earth, which, at core depths, is known only to within a few thousand degrees! It is therefore the challenge of the next few years among deep-Earth scientists to develop accurate measurements and models of the properties of the high-pressure silicates and iron alloys at deep-Earth conditions. With an interdisciplinary approach involving theory, experiment and seismology we will be able to determine the nature, evolution and influence of the Earth's deep interior.

Keywords: mineral physics; experimental petrology; computer simulation; high P/T; Earth's mantle; Earth's core

1. Introduction

The Earth upon which we live is a poorly understood planet. We live on its surface, drill into its crust, and are mere observers of remarkable natural phenomena such as the volcanic eruptions that occur close to plate boundaries. The material that we can sample directly in this way has come from only a few hundred kilometres down into the Earth; there remain well over 6000 km to go before the centre is reached. The only way in which we can explore the deep interior directly is by observing seismic waves that travel through the Earth, generated after earthquakes. By analysing these waves, seismologists have built up a picture of the gross structure of the Earth's interior (figure 1); this shows it to be layered with significant seismic-wave velocity discontinuities at the boundaries between the different layers: the crust, the upper mantle, the transition zone, the lower mantle, the liquid outer core, and the solid inner core. Beneath the complex crust lies the mantle, made up of silicate rock, and the core, which is mostly iron alloyed with *ca.* 10% light elements.

Ideas about the nature of the Earth's interior have developed significantly over recent years. Perhaps the greatest single advance in geological thought during the 20th century was the development of plate tectonic theory. This elegant model explained the existence and topography of the Earth's oceans and continents, the relative motions of the continents, the compositional variations seen in volcanoes from different tectonic settings, and demonstrated the main mechanism for heat loss in the Earth. However, many challenges remain in our understanding of Earth processes as we enter the 21st century—the nature of the convective regime in the deep mantle and core; the nature of material and heat transport across the boundary zone between the upper and lower mantle; the thermal profile of the lower mantle; and the nature of thermal, mechanical and electromagnetic coupling across the core–mantle boundary—these are all intimately tied up with the physical properties of

the Earth's high-pressure minerals. The Earth's core is even less well understood and many questions remain unanswered, such as the nature of the crystalline structure of the inner core, which is crystallizing out from the liquid outer core, the origin of the seismically observed inner-core anisotropy, the temperature of the inner core–outer core boundary, the light elements in the core, and the dynamical processes governing convection in the outer core, which leads to magnetic-field generation.

The experimental and theoretical techniques that have been used to probe our planet have developed significantly over recent years. Current developments in *in situ* high-pressure experimental techniques, the rapid advances made by *ab initio* modellers, and a cross-disciplinary approach combining these with solid-Earth geophysical methods hold the key to solving these major questions of Earth evolution. While the experimentalists continue to gain access to higher temperatures and pressures, computational mineralogy is fast becoming the most effective and quantitatively accurate method for successfully determining mineral structures, properties and processes at the extreme conditions of the Earth's deep interior. Using a variety of simulation techniques, theorists are not only able to provide a microscopic underpinning to existing experimental data, but also provide a sound basis from which to extrapolate beyond the limitations of current experimental methods. The physical and chemical properties of candidate Earth materials obtained by both theoretical and experimental methods may be compared with those inferred from seismic observations, and so used to constrain the composition and thermodynamic evolution of the Earth's deep interior. In this paper, we shall first outline the experimental and theoretical techniques that are currently being used to determine the properties of deep-Earth materials; we shall then review some of the recent advances in our understanding of the Earth's deep interior using these methods; and, finally, we shall discuss the major challenges facing Earth scientists as we enter the new millennium.

2. Experimental techniques

The Earth's deep interior cannot be readily accessed for study; however, it is possible to produce, experimentally, the high-pressure and high-temperature conditions of the Earth's interior and observe their effects on minerals. The aim of the experimentalist is to achieve these conditions of very high pressures and temperatures with the greatest accuracy and precision, and then probe the microstructure of the samples looking for clues as to what compositions and processes dominate in the Earth's deep interior.

The two main approaches used to generate ultra-high pressures in the laboratory are static loading and shock loading. Static loading uses hard anvils to compress the sample, often amplifying the applied pressure by tapering the anvil to reduce the surface area of sample that supports a fixed load. In shock loading, a high-velocity projectile is fired at the sample and the impact shock wave generates ultra-high pressures and temperatures in the sample for durations of milliseconds or less. Overviews of high-pressure experimental techniques are given in Holloway & Wood (1988) and Mao & Hemley (1998); however, the two examples below demonstrate the principles of high-pressure and high-temperature generation.

(*a*) *Static compression*

The simplest and most elegant of the tapered anvil devices is the diamond-anvil cell (see Mao & Bell (1975) and figure 2). Diamond is transparent to electromagnetic

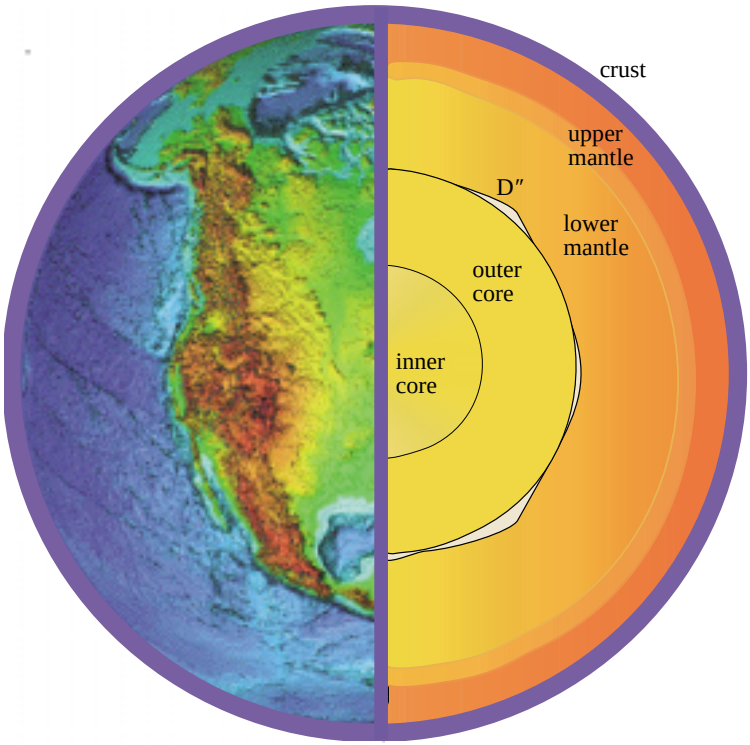

Figure 1. Schematic view of the Earth's interior depicting the seismically determined layers. The crust and mantle are composed of solid silicate and oxide minerals. The mantle is subdivided by seismic discontinuities into upper mantle (less than 410 km deep), transition zone (410–670 km) and lower mantle (670–2890 km). The liquid-iron outer core (2890–5150 km) contains *ca.* 10 wt% of light alloying elements and the solid-iron inner core extends to the Earth's centre at a depth of 6371 km. The D″ zone at the base of the lower mantle has complex topography ranging from a few tens to hundreds of kilometres thickness, and is thought to be the result of reaction between the metallic core and silicate mantle.

radiation from the far infrared through visible and ultraviolet into the hard X-ray region. Therefore, in addition to direct observation of pressure- and temperature-induced phase transitions, these devices are ideal for a wide range of spectroscopic and diffraction-based techniques.

Pressure is generated by applying a small load to the backs of two opposing gem-cut diamonds using hand screws or low-pressure gas bellows. The small pressure on the back of the diamonds is amplified many times at their tips, which have a truncated area of 0.2 mm^2 or less. A toroidal gasket, consisting of a hard metal foil with a small hole located axially to the diamonds, stops the pressure medium from extruding and seals the sample environment. The volume at high pressure, typically 10^{-3} mm^3, is compressed uniaxially by the diamonds. Within this high-pressure volume, a pressure medium (liquid methanol–ethanol mixture for low P/T, or high-density gas for high P/T) surrounds the sample (*ca.* 10^{-4} mm^3) and exerts a hydrostatic pressure. Pressure is calibrated against the cell parameters of a sample with a well-known equation of state, which sits in the pressure medium alongside the

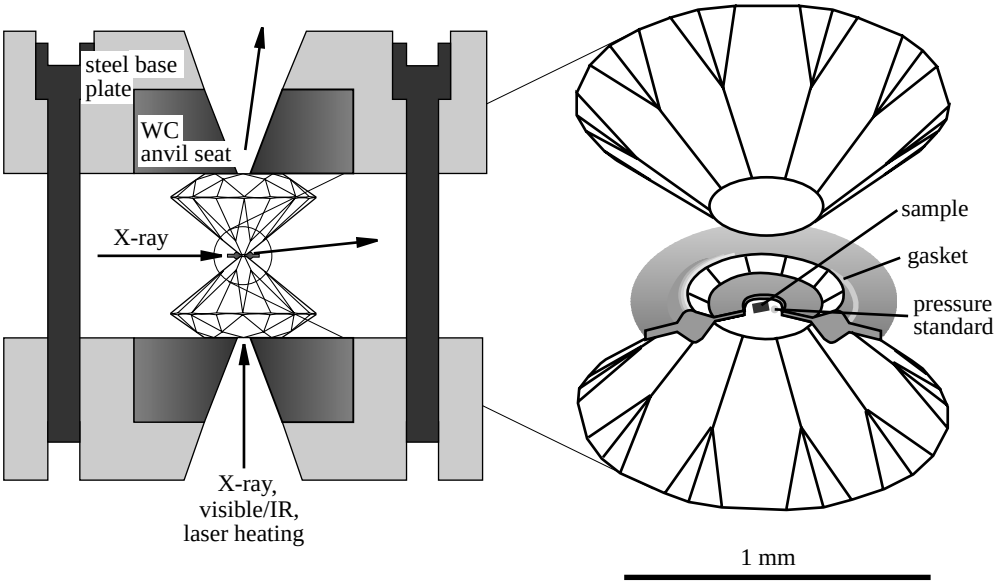

Figure 2. The diamond-anvil cell. Force is applied to the back of the diamonds by tightening the screws connecting the base plates. The diamonds compress the small sample volume between their tips and the metal gasket, shown in the enlargement. The sample and a pressure standard are surrounded by a soft pressure medium and experience nearly perfect hydrostatic pressure. The excellent transparency of diamond to many wavelengths of light allows many spectroscopic and diffraction-based studies to be performed in the diamond cell.

experimental sample of interest. In this way, pressures in excess of 300 GPa can be obtained in the diamond cell (Mao *et al*. 1989; Liu & Vohra 1996).

In the diamond-anvil cell, the sample can be heated using a resistive furnace placed around the diamonds, and the temperature measured using thermocouples close to the diamond tip. Resistive heating is limited by the stability of diamond and softening of load-bearing components to less than 1000 K; however, for higher temperatures, the sample can be heated directly by laser. The laser light passes through the diamond and is absorbed by the sample, thus avoiding undue heating of the diamonds. Temperatures in excess of 4000 K can be obtained by laser heating. Early problems of high thermal gradients and attendant temperature uncertainties have been solved by use of mixed-focusing modes and heating from both sides (see, for example, Manga & Jeanloz 1998; Shen *et al*. 1998*a*). Temperature is measured from the black-body radiation spectrum for the sample with a quoted accuracy of 1–10%.

(*b*) *Shock compression*

A light-gas gun (see, for example, Ahrens 1980) is used to generate pressures to the terapascals range for a duration of milliseconds. The P–T–t path of the sample is complex, depending on sample and capsule geometry, density and shock impedance, and mass and velocity of the impactor. The ultra-high pressure range achieved, however, renders these experiments vital for studying compression and phase changes at the conditions of the Earth's deep lower mantle and core.

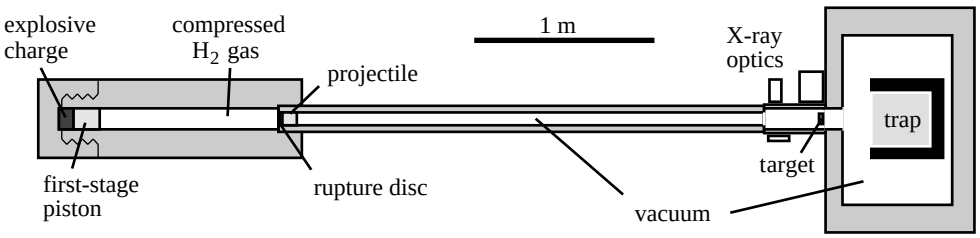

Figure 3. The double-stage light-gas gun can generate ultra-high pressures and temperatures in range of terapascals and kilokelvins for durations of up to milliseconds. The experiment is initiated by igniting the charge, which drives the piston along the first stage (large-bore) barrel. The H_2 gas is compressed by the piston until the disc connecting the first and second stage barrels ruptures. The expansion of the gas accelerates the projectile along the second stage (small-bore) barrel and into the sample at velocities of several kilometres per second. The resultant shock wave generates ultra-high pressures with adiabatic heating in the sample. Fragments of the sample can be collected in the trap for later analysis. The projectile velocity is measured using two beams of light, which cross its path with a precisely known spacing. Shock velocity is measured using mirrors connected to the sample and a high-speed film.

A two-stage light-gas gun (figure 3) consists of two long gun barrels connected end to end via a solid disc that is designed to rupture at a critical pressure. The small-bore portion contains the projectile, adjacent to the rupture disc, and opens in to the evacuated sample chamber. The first-stage propellant explosive is placed at the far end of the large-bore barrel behind a light piston. The experiment is initiated by igniting the explosive, which accelerates the piston down the large-bore tube and compresses a light gas between the piston and the rupture disc. When the disc ruptures, the gas expands into the small-bore barrel, accelerating the projectile before it. The maximum attainable velocity is determined by the rate at which the gas can expand, hence the use of a light gas, usually H_2. The projectile exits the small-bore barrel and impacts the sample, causing a high-pressure shock wave with adiabatic heating and subsequent low-pressure release wave, which normally causes the sample to fragment. The velocities of the projectile and shock wave are measured optically and temperature can be measured from the black-body radiation spectrum.

(*c*) *Developments in in situ techniques*

The development over recent decades of *in situ* techniques to measure a range of physical properties at high experimental pressures and temperatures has opened a whole new vista for the deep-Earth sciences. Optical (see, for example, Manghani *et al*. 1998) and γ-ray spectroscopy (Pasternak *et al*. 1997) in the diamond cell provide powerful probes of the electronic and nuclear environment of samples, while X-ray diffraction in the diamond cell has been the workhorse of high-pressure crystallographers determining crystal structures and equations of state for several decades. Electrical conductivity measurements with electrodes passing through the gaskets (Li & Jeanloz 1991; Shankland *et al*. 1993) or embedded within the diamond anvil (Catledge *et al*. 1997), or in the larger volume multi-anvil press (Omura 1991; Dobson *et al*. 1997; Xu *et al*. 1998*a*, *b*), allow *in situ* measurements of mobilities of various species within minerals and provide important constraints for interpreting

geomagnetic-field measurements in terms of electrical, thermal and chemical structure within the deep Earth.

It is, however, the advent of synchrotron radiation sources with dedicated high-pressure beamlines that will most revolutionize high-pressure experiments in the coming decades. The new, high-brightness, third-generation synchrotron sources will allow *in situ* high-P/T X-ray absorption spectroscopy (XAS) experiments, a vital tool for probing short-range structural and electronic interactions between neighbouring atoms.

Synchrotron-based X-ray diffraction in both diamond-anvil and multi-anvil cells allows rapid mapping of P/T stability and structural refinement of non-quenchable minerals. The addition of diffraction-based pressure standards to the sample allows very accurate determinations of phase boundaries, which is particularly important for comparing pressure-induced mineralogical phase changes with seismic discontinuities (Irifune *et al*. 1998). Simultaneous measurements of ultrasonic-sound-wave velocity with diffraction will increase our precision in equation-of-state (EOS) studies by orders of magnitude and will allow quantitative measurements of the high-order terms that are vital for mapping mineral compression across the pressure range encountered within the Earth. Additionally, the speed at which spectra can be collected from synchrotron sources facilitates studies of the kinetics of phase transformations at high P/T.

Recent studies using the broadening of diffraction peaks have been reported which enable the measurement of elastic strain in olivine (Weidner *et al*. 1998) and its high-P/T annealing in a multi-anvil press. This will be an important technique for studying plastic deformation in deep-Earth minerals over the coming decades.

X-ray shadowgraphy techniques measure differences in X-ray absorption across the sample volume. This has been used to image dense falling spheres in high-pressure viscosity measurements, based on Stokes's law (Kanzaki *et al*. 1987; Dobson *et al*. 1996). Additionally, measuring X-ray absorption from a sample of known thickness provides a precise measure of density (Katayama *et al*. 1993). The background from the pressure medium can be filtered out by comparing the absorption from varying thicknesses of sample. This technique promises to be particularly useful for measuring the density of liquid metals and other dense amorphous phases.

Despite the rapid advances being made, there are limits to experimental investigations; for example, it is generally very difficult to establish the detailed microscopic atomistic and electronic mechanisms involved in thermoelastic and dynamic processes simply from experimental study. Furthermore, even though diamond-anvil and multi-anvil cell techniques have advanced dramatically, the experimental study of minerals under core conditions is still a major challenge. As a result, therefore, in order to complement existing experimental studies and to extend the range of pressure and temperature over which we can model the Earth, computational mineralogy has, in the past decade, become an established and growing discipline.

3. Computational methods

The simulation techniques used to model minerals and the processes occurring within the Earth's deep interior generally fall into the categories: *atomistic simulations*, using potential models to describe the interactions between atoms, and *quantum-mechanical simulations*, calculating electronic structure from first principles. In the

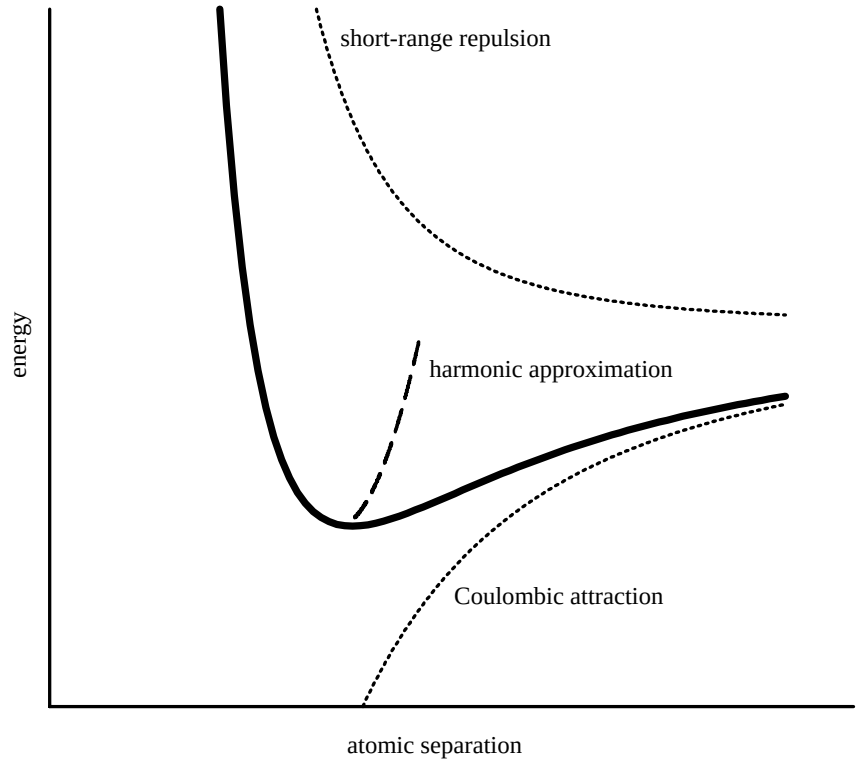

Figure 4. Energy as a function of atomic separation with both the attractive and repulsive components; at higher temperatures, the atoms vibrate anharmonically, away from the harmonic approximation.

first case, the energy of the system is written in terms of an atomistic potential function, the parameters for which may be determined either experimentally or from first principles; in the second case, the energy of the system is written in terms of electronic interactions, where appropriate substitutions are made in order to solve the Schrödinger equation for the system. In the latter case, no empirical input parameters are required and an exact solution is found. The chosen technique depends upon the system and process simulated and the level of approximation required. By setting up on a computer an artificial simulation box of particles, whose energy is governed by either an atomistic or quantum-mechanical potential, calculations may be performed in order to predict how these systems respond to high pressures and temperatures.

(*a*) *Simulations using atomistic potential models*

The interatomic potential gives the energy of interaction between the atoms or ions within a system as a function of their separations and orientations. When no net forces are acting on the constituent atoms, the sum of the attractive and repulsive potential energies between each pair (ij) of atoms in a crystalline solid at 0 K is

termed the static lattice energy:

$$U_0(\boldsymbol{r}_{ij}) = \sum_{ij} \frac{q_i q_j}{\boldsymbol{r}_{ij}} + \sum_{ij} \varphi_{ij} + \sum_{ijk} \theta_{ijk}. \tag{3.1}$$

The three terms on the right-hand side represent the contribution to the static lattice energy from the long-range Coulombic attraction, a repulsive term due to the diffuse nature of the electron clouds surrounding the nucleus, and an optional three-body term that takes into account non-pairwise interactions (figure 4).

The optimum potential function that describes interactions between atoms in a given system is obtained either empirically or from first principles. Once the system has been set up, 0 K structural data may be obtained from the first derivative of the potential function. However, in order to successfully model deep-Earth mineral phases, it is desirable to simulate conditions of extreme pressure and temperature. Modelling static pressure is fairly straightforward, being derived from the forces between the atoms, which are obtained from the first derivative of the potential function. However, modelling temperature (and the associated kinetic pressure due to atomic vibrations) requires more sophisticated techniques. The techniques that have been developed in order to achieve this include

(i) *lattice dynamics*, where the system is described in terms of atomic lattice vibrations (phonons) each with a wavelength, λ, and a frequency, ω (see, for example, Cochran 1973); and

(ii) *molecular dynamics*, where the atoms are given initial positions and velocities that are allowed to evolve over a period of time via solutions to Newton's equations of motion (see, for example, Allen & Tildesley 1987).

(i) *Lattice dynamics*

The lattice-dynamics method is a semi-classical approach that describes the system in terms of a simulation box containing harmonic oscillators whose frequencies vary with cell volume. The motions of the individual particles are treated collectively as lattice vibrations or phonons (figure 5*a*). The phonon frequencies may be calculated from analysis of the forces between the atoms, and many thermodynamic properties, such as free energies, may be calculated using standard statistical mechanical relations, which are direct functions of these vibrational frequencies. For example, the Helmholtz free energy may be written

$$F_{\text{total}} = U_0 + F_{\text{vibrational}}, \tag{3.2}$$

where U_0 is the static lattice energy (equation (3.1)) and $F_{\text{vibrational}}$ is given by

$$F_{\text{vibrational}} = k_{\text{B}} T \sum_i \left(\frac{h\omega_i}{2k_{\text{B}}T} + \ln(1 - \mathrm{e}^{h\omega_i/(k_{\text{B}}T)}) \right). \tag{3.3}$$

Therefore, since k_{B} and h are Boltzmann and Planck constants, respectively, the thermal contribution to the free energy at some desired temperature is a function only of the phonon frequencies, ω_i. Similar relations may be obtained for many other thermodynamically important quantities, each expressed as a function of ω_i.

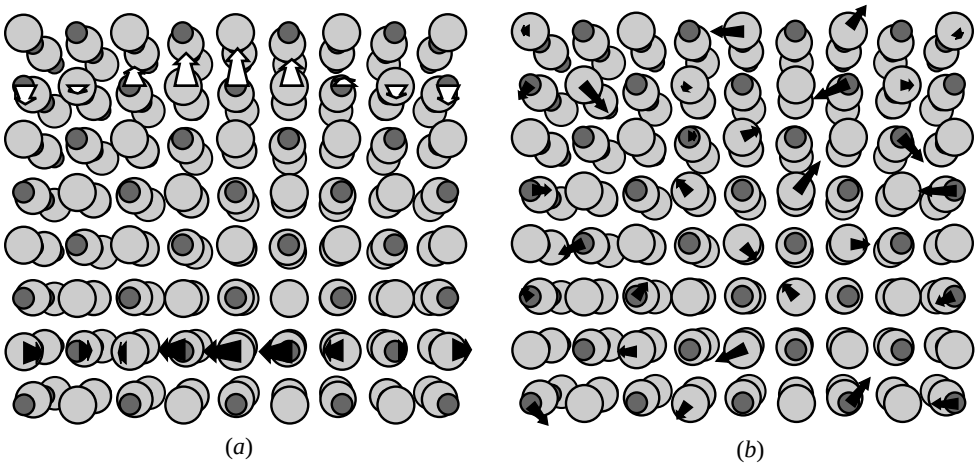

Figure 5. Schematic simulation boxes for lattice dynamics (*a*) and molecular dynamics (*b*). (*a*) In a lattice-dynamics calculation, at low simulated temperatures, the motion of the individual particles are treated collectively as a vibrational wave (phonon) in the crystal. (*b*) Molecular-dynamics simulations, which take into account the explicit motion of individual particles in the simulation box, are more appropriate for high-temperature simulations since they allow for high-temperature anharmonicity.

A limitation of the lattice-dynamics method is that it treats the atoms as harmonic oscillators, whereas at very high T, the oscillations become anharmonic as their displacements from equilibrium become asymmetric (as seen in figure 4), so another treatment is required to take this into account.

(ii) *Molecular dynamics*

Molecular dynamics is routinely used for medium- to high-temperature simulations of minerals in which atomic vibrations become more anharmonic. The interactions between the atoms within the system are described in terms of the potential model discussed earlier, but, instead of treating the atomic motions in terms of lattice vibrations, each ion is treated individually. Molecular-dynamics methods are described in detail in Allen & Tildesley (1987), and outlined in the context of applications to the Earth in, for example, Vočadlo *et al.* (1995). In principle, Newton's equations of motion are solved for a number of particles within a simulation box to generate time-dependent trajectories and the associated positions and velocities that evolve with each time step (figure 5*b*). Here, the kinetic energy, and, therefore, the temperature, are obtained directly from the velocities of the individual particles. With this explicit particle motion, the anharmonicity is implicitly accounted for at high temperatures. Molecular-dynamics methods may also be used to simulate liquids, and are, therefore, the preferred method when simulating liquid-iron alloys at the conditions of the outer core.

The shortcomings of both lattice dynamics and molecular dynamics lie in their dependence upon the accuracy of the chosen potential model, which, in turn, is limited by the ability of such a potential to describe anything other than closed-shell systems. Ideally, we would like to model deep-Earth mineral phases without any recourse to empirical parametrization. This *ab initio* approach is becoming increas-

ingly routine for the simulation of simple systems and simple processes, and is currently being developed to successfully model complex structures with ionic, covalent and metallic bonding under extreme conditions of pressure and temperature.

(*b*) *Ab initio quantum-mechanical simulations*

Quantum-mechanical simulations were first employed by Car & Parrinello (1985) and are based on the description of the electrons within a system in terms of a quantum-mechanical wave function, $\psi(\boldsymbol{r})$. Although not directly observable itself, the square of this wave function, $|\psi(\boldsymbol{r})|^2$ gives the probability of finding an electron at any point $\boldsymbol{r}$. The energy and dynamics of a single electron are governed by the general Schrödinger equation for a non-relativistic single particle of mass m in free space:

$$E\psi = -\frac{\hbar^2}{2m}\nabla^2\psi. \tag{3.4}$$

However, in minerals we do not have single particles in free space, but instead many bound electrons that interact with both the ionic nuclei and with each other. This poses a serious problem as the wave function for a system containing more than one electron is not just a product of one-electron wave functions, but a very complex many-electron wave function,

$$E\Psi(r_1, r_2, \ldots, r_N) = \left(-\frac{\hbar^2}{2m}\nabla^2 + V_{\text{ion}} + V_{\text{e–e}}\right)\Psi(r_1, r_2, \ldots, r_N), \tag{3.5}$$

where the perturbation to the energy of the electron in free space (equation (3.4)) may be expressed in terms of an ionic contribution and a Coulombic contribution (the second and third terms within the brackets of equation (3.5)) summed over all electronic wave functions. In principle, once the wave function for a system has been determined, energy minimization techniques may then be applied in order to obtain the equilibrium structure for the system under consideration.

Unfortunately, the complexity of the wave function, Ψ, means that this type of problem cannot be readily solved. However, there are a number of approximations that may be made to simplify the calculation, whereby good predictions of the structural and electronic properties of materials can be obtained by solving, self-consistently, the one-electron Schrödinger equation for the system, and then summing these individual contributions over all the electrons in the system. Such approximation techniques include density functional theory (DFT) (Hohenberg & Kohn 1964), whereby the average electrostatic field surrounding each electron is treated similarly, reducing the many-body Hamiltonian in the Schrödinger equation to that for one electron surrounded by an *effective* potential associated with the interactions of the surrounding crystal. However, the electron is not in an average field because there is *correlation* between the electrons, and also electronic spin (the *exchange*), governed by Pauli's exclusion principle, both of which serve to reduce the energy of the system. In DFT, each electron sits in an effective potential and an approximation is made for the electronic exchange and correlation. There are a number of ways of implementing this approximation using a variety of techniques (see Singh (1994) for details).

Once the energy of the system has been calculated, the interatomic forces may then be obtained, which, when combined with classical lattice-dynamics or molecular-dynamics techniques, may be used to calculate thermoelastic and related dynamic

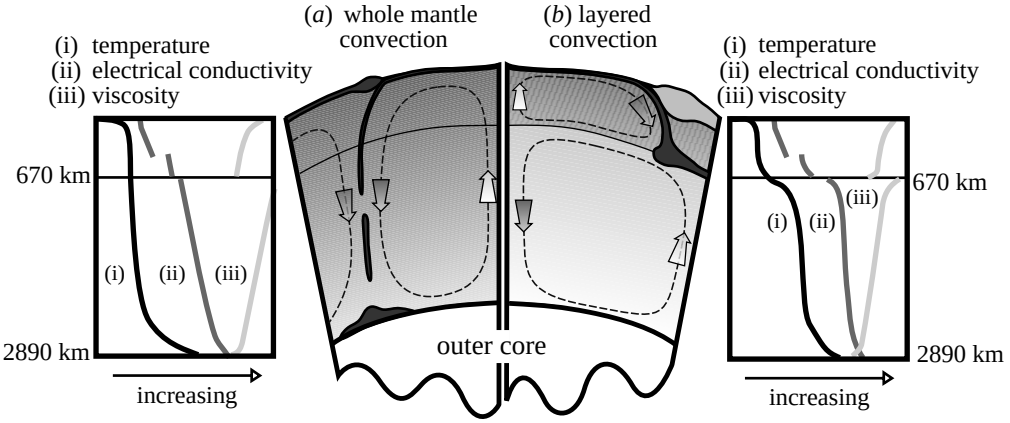

Figure 6. Schematic of whole-mantle (*a*) and layered (*b*) convection; dashed lines represent flow streamlines with arrows in flow direction. Inferred temperature (i), electrical conductivity (ii) and viscosity (iii) are plotted against depth for both scenarios. (*a*) In whole-mantle convection, the 670 km seismic discontinuity is due solely to phase transformations to high-pressure polymorphs. There is no mid-mantle thermal discontinuity, with an adiabatic thermal gradient between 200 and 2000 km. Large increases in viscosity and electrical conductivity at 670 km (and 410 km) depth are postulated due to olivine–spinel and spinel–perovskite plus magnesiowüstite phase changes. (*b*) Layered-convection models imply that there is little mass transfer across 670 km, with the upper and lower mantle convecting as separate systems. This results in the upper and lower mantle having separate compositions and a large superadiabatic thermal gradient in the mid-mantle where heat is transferred from the lower mantle to the upper mantle by conduction. Increased lower-mantle temperatures, relative to the whole-mantle model, result in increased electrical conductivity and reduced viscosity in the lower mantle.

properties such as free energy, mentioned above. In first-principles calculations, electronic contributions to energies must be included explicitly, so, in the example given earlier (equation (3.2)), the Helmholtz free energy, must now be written as

$$F_{\mathrm{total}} = U_0 + F_{\mathrm{vibrational}} + F_{\mathrm{electronic}}, \tag{3.6}$$

where the electronic contribution to the free energy is calculated from DFT. Using these techniques, it is possible, in principle, to simulate any desired mineral at pressures and temperatures existing throughout the entire Earth. Such calculations are time consuming and CPU intensive, but, with increasingly powerful supercomputers, these calculations are being performed on ever bigger and more complex systems.

4. Probing the Earth's deep interior

Using the experimental and theoretical techniques outlined above, it has been possible to probe the Earth's deep interior with increasing accuracy and precision. Although we cannot detail every advance in recent years, we shall outline some of the major research challenges of interest to geoscientists today.

(*a*) *The Earth's mantle*

The minerals that exist and the processes that occur in the Earth's mantle are determined by the thermodynamics of the deep interior. Heat, generated within

the Earth by exothermic crystallization of the liquid outer core and by radioactive decay, is transported to the surface mainly by slow convection in the mantle, which, over geological time-scales, flows plastically. Oceanic crust is constantly being generated at up-welling regions of the mantle convection cells and being destroyed at subduction zones, where it is dragged deep into the mantle on down-welling convective limbs (figure 6). One of the major problems associated with the Earth's mantle is understanding what happens to these subducting slabs. There is considerable debate over whether the subducted oceanic crust continues down to the core–mantle boundary or ponds on top of the denser lower mantle. A mid-mantle reservoir of subducted material would indicate that convection within the mantle occurs in separate upper and lower-mantle cells, with little mass transfer across the boundary and separate compositions in the upper and lower-mantle cells. Furthermore, heat would be transferred across the boundary layer by conduction, resulting in a superadiabatic thermal gradient of 1000 K or more. Conversely, if material is subducted to the core–mantle boundary, then the mantle convects as a single cell with good chemical mixing between upper and lower mantle.

Multi-array seismic studies—for example, the Preliminary Reference Earth Model (PREM) (Dziewonski & Anderson 1981)—clearly demonstrate that at 410 km and 670 km depth within the Earth's mantle there are discontinuities in density (of 5% and 10%, respectively), P-wave (2.5% and 4.7%) and S-wave velocity (3.3% and 6.8%), which pervade the globe with relatively little variation in depth. These discontinuities may be produced by a change in composition, or by a change in mineralogy to denser high-pressure phases. Early high-pressure phase relation studies showed phase changes in Mg_2SiO_4 from olivine to wadsleyite, ringwoodite and, finally, to $(Fe,Mg)SiO_3$ perovskite plus (Fe,Mg)O magnesiowüstite with increasing pressure. The pressures of the transitions olivine–wadsleyite and ringwoodite–perovskite plus magnesiowüstite agree with the 410 km and 670 km depths given the appropriate geotherm; however, the presence of phase transitions at the appropriate depth does not preclude the possibility of compositional variations as well.

Current seismic imaging studies suggest that the subducting slab can penetrate or can be deflected by the 670 km discontinuity (Christensen 1996), and also that, within the cooler subducted slab, the 410 km and 670 km discontinuities are displaced upwards and downwards, respectively, consistent with the P/T stability slopes of the olivine–wadsleyite and ringwoodite–perovskite plus magnesiowüstite reactions. The composition of intra-plate hot-spot related volcanism suggests, however, that the deep source of these magmas has a different chemical composition from the mid-ocean-ridge (upper mantle) source.

Recent fluid-dynamical simulations of mantle convection (see, for example, Peltier & Solheim 1992; Glatzmaier & Schubert 1993), which include the phase changes at 410 km and 670 km, suggest that the convection within the Earth's mantle periodically switches between stable modes of two-layer convection to convective overturn during which there is significant mass and heat transfer across 670 km. These geophysical simulations are sensitive estimates of mineral properties, in particular their viscosity. For example, the ability of a subducting slab to penetrate the density barrier at 670 km depends on the relative strength of olivine and perovskite. We have a qualitative understanding of the strength of mantle minerals; we know that heat weakens minerals, so a 1000 K mid-mantle thermal discontinuity would significantly reduce lower-mantle viscosity, and we also know that the high-pressure perovskite

phase is significantly stronger than upper-mantle phases. Recent results from diffusion experiments (Chakraborty *et al.* 1999) suggest, counterintuitively, that wadsleyite in the transition zone, between 410 km and 670 km depth, may be weaker than either olivine or perovskite.

Improvements in simulation speed and accuracy allow accurate calculation of P–V–T equations of state in perovskite and magnesiowüstite (Yagi & Funamori 1996; Da Silva *et al.* 1999). Comparing these with the density profile derived from seismic studies (Dziewonski & Anderson 1981) shows (i) that there is a significant superadiabatic thermal gradient, of 1000 K or more, towards the base of the lower mantle; and (ii) a lower and upper mantle of the same composition produce geotherms consistent with whole-mantle convection, whereas a lower mantle significantly enriched in silica is consistent with a 1000 K discontinuity at 670 km and, therefore, with layered convection.

The electrical conductivity of mantle minerals provides an independent test for mantle geotherms derived from the EOS studies (Dobson & Brodholt 1999). Temporal variations in the geomagnetic field can be related to the Earth's electrical conductivity profile (by isolating the internal component of the field variations and treating the Earth as a series of spherical shells of varying conductivity (see, for example, Parker 1970)). Experimental electrical conductivity measurements of the major mantle phases, olivine, wadsleyite, ringwoodite, perovskite and magnesiowüstite (Dobson *et al.* 1997; Xu *et al.* 1998*a*, *b*; Katsura *et al.* 1998) can be used to predict the Earth's electrical conductivity profile, given an assumed geotherm. The electrical conductivity of the lower mantle depends on temperature, and the ferric iron content and equilibrium geometry of perovskite and magnesiowüstite. Laser-heated diamond-anvil cell experiments (Martinez *et al.* 1997) suggest that, at textural equilibrium, the more conductive magnesiowüstite forms isolated grains enclosed by perovskite and so would not significantly contribute to lower-mantle conductivity. Recent experiments (Wood & Rubie 1996; McCammon 1997) and calculations (Richmond & Brodholt 1998) suggest that the ferric iron is controlled by aluminium solution in perovskite. Geochemical arguments suggest that the lower mantle contains *ca.* 3 wt% alumina, which would produce a lower-mantle perovskite composition of around $(Mg_{0.91}Fe^{2+}_{0.07}Fe^{3+}_{0.02})(Al_{0.02}Si_{0.98})O_3$. The high ferric iron results in a highly conductive perovskite, which requires a cool lower-mantle geotherm to be consistent with the geomagnetic response. If, on the other hand, the lower mantle was depleted in iron or aluminium, or the aluminium resided in a separate volumetrically minor phase, a hot lower mantle would be necessary for an electrical conductivity profile consistent with the geomagnetic response.

(*b*) *The core–mantle boundary*

The changes in chemical and physical environment between the Earth's core and mantle are as great as any in the Earth. Density and seismic velocity changes across the core–mantle boundary (CMB) are more than one order of magnitude larger than across the 410 km and 670 km seismic discontinuities combined. The change from solid-silicate lower mantle to liquid-metal outer core entails a change in physical state and chemistry as profound as the atmosphere–geosphere boundary. As well as the major radial variations, the CMB shows strong lateral heterogeneities. The CMB is intimately connected to evolution of the Earth through the heat transfer and magnetic coupling between outer core and mantle.

Seismic studies of the CMB suggest that the base of the lower mantle is highly complex (see, for example, Loper & Lay 1995; Wysession 1996), with zones of seismic anisotropy, seismically slow zones and seismic discontinuities. These regions have a complex topography that may be controlled by mantle convection cells. Seismic anisotropy can be explained by preferential alignment of minerals equilibrating with local stress fields (Karato *et al*. 1995; Stixrude 1998). The seismically slow zone in the bottom 150–450 km of the mantle has been interpreted as due to partial melting (see, for example, Stixrude & Bukowinski 1990; Wysession *et al*. 1998). Seismic discontinuities require rapid variations in density that may be due to infiltration of outer core material into, and reaction with, the lower mantle (see, for example, Jeanloz & Williams 1998), ponding of subducted oceanic lithosphere (see, for example, Wysession 1996; Kendall & Silver 1998), or partial melting of the lower mantle (Stixrude & Bukowinski 1990).

In spite of its complexity and importance, the CMB is very poorly understood. The large density contrast between core and mantle acts as a barrier to significant mass transport between core and mantle. The resulting large superadiabatic thermal gradient at the base of the lower mantle is seen in EOS-based geotherms (Yagi & Funamori 1996; Da Silva *et al*. 1999). Despite this, the temperature of the CMB is very poorly constrained. Phase equilibria provide P/T anchor points at the solid–liquid phase change at the inner-core boundary and the spinel–perovskite plus magnesiowüstite transition at 670 km; however, temperature estimates at the CMB rely on extrapolations upwards from the inner-core boundary or downwards from 670 km. A large superadiabatic temperature increase near the CMB would be gravitationally unstable unless the density of the lower-mantle material increased in this region.

Another important result of the CMB mass transport barrier is that the outer core and lower mantle may well be significantly out of chemical equilibrium. Chemical reactions between core and mantle materials have been studied in laser-heated diamond cells (Knittle & Jeanloz 1989; Goarant *et al*. 1992; Poirier *et al*. 1998) and have been shown to involve solution of iron and oxygen into the liquid metal leaving solid FeSi and iron-poor silicate residues. In addition, there may be loss of some of the core alloying elements to the mantle as iron is extracted from the outer core by crystallization causing enrichment of the alloying light elements. The resulting mixture of iron alloys and Fe-depleted mantle silicates at the base of the lower mantle might explain the observed anomalous seismic behaviour and provide the necessary density to support a superadiabatic deep lower mantle, but high-pressure EOS and acoustic-velocity measurements are yet to be performed on these materials.

(*c*) *The Earth's core*

The Earth's core occupies approximately half of the planet by radius, yet the conditions of pressure (above 135 GPa) and temperature (*ca.* 3000–7000 K) make it very difficult to study experimentally. The core is predominantly made up of iron with some lighter alloying elements. In order to understand the core, we would ideally like to have information on all multiphase systems containing iron and candidate lighter elements at core conditions. However, even the high-P/T behaviour of *pure* iron presents major problems, which must be resolved before the more complex phases can be properly understood. Therefore, the physical properties of iron and its alloys are of considerable interest to Earth scientists.

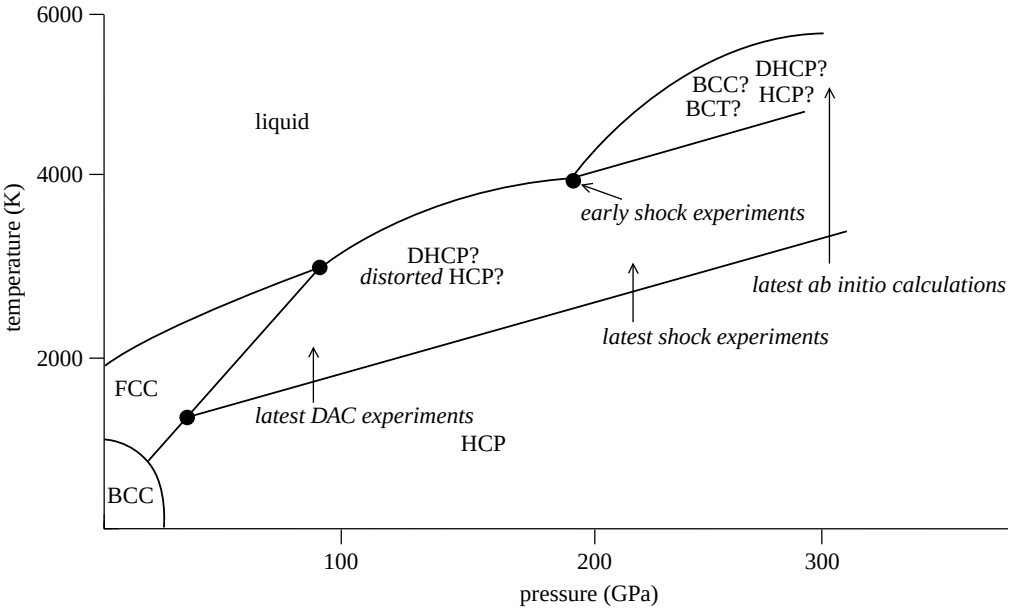

Figure 7. Schematic of the phase diagram of pure iron at high pressures and temperatures, based on current experimental and theoretical results. Crystal structures are: BCC (body-centred cubic); FCC (face-centred cubic); HCP (hexagonal close-packed); BCT (body-centred tetragonal); DHCP (double-hexagonal close-packed). The phase diagram is well constrained at low pressures and temperatures, where a range of different experimental techniques give consistent results, but, at higher P/T conditions approaching those of the core (130–310 GPa; 3000–7000 K), there is still considerable controversy over the phase diagram of iron.

(i) *The crystalline structure of iron in the inner core*

The inner core is crystallizing out of the liquid outer core, and knowledge of the melting curve for iron at these very high pressures and temperatures would place considerable constraints on the temperature at the inner-core–outer-core boundary. Direct experimentation on Fe at core pressures (up to 360 GPa) and temperatures (up to 7000 K) has yet to be achieved; even at experimentally accessible conditions ($P < 200$ GPa, $T < 3000$–4000 K) there are major conflicts between the results of different groups (figure 7). In particular, the possibility of a solid–solid phase transition from HCP to a structurally ill-defined β-phase has been observed above *ca.* 35 GPa and *ca.* 1500 K through *in situ* X-ray diffraction experiments (Andrault *et al*. 1997; Saxena *et al*. 1996; Boehler 1993). It has been suggested that the crystal structure of this phase could be DHCP-Fe (Saxena *et al*. 1996) or an orthorhombically distorted HCP polymorph (Andrault *et al*. 1997). However, more recent *in situ* X-ray diffraction experiments by another group have observed no such phase transition (Shen *et al*. 1998*b*) with HCP-Fe remaining stable at high P and T until the onset of melting. Moreover, the existence of another solid–solid phase boundary above *ca.* 200 GPa and *ca.* 4000 K has been suggested to reconcile data from static and shock experiments (Anderson & Duba 1997). Although the structure of this phase is unknown, it has been suggested that it might be BCC-Fe (Bassett & Weathers 1990); this is supported by classical molecular-dynamics calculations (Matsui 1993), but the results

of such calculations are hampered by the validity of using parametrized potentials beyond the range of their empirical fitting. However, successful first-principles calculations have already been performed on iron (see, for example, Vočadlo *et al*. 1997), and, for the first time, *ab initio free energy* calculations have been performed on all the suggested candidate phases for the core at core conditions (Vočadlo *et al*. 1999). The results show that iron undergoes no mid–high-P/T phase change and remains hexagonally close-packed at inner-core conditions, consistent with new results from the latest very-high-P/T shock experiments (Nguyen & Holmes 1998).

(ii) *Inner-core anisotropy*

The inner core is known to be anisotropic from the presence of seismic travel-time anomalies in the core region, but the origin of this anisotropy is unknown. It may be due to small heterogeneities within the core, or intrinsically due to the possible anisotropic structure of the crystalline core material. The latter explanation is often favoured because it is thought that pure iron exhibits elastic anisotropy at core conditions. A polycrystalline aggregate of iron will have less anisotropy than that of a pure crystal, so it is important to know the magnitude of elastic anisotropy in iron in order to constrain the preferred alignment in the inner core. *Ab initio* calculations on the elastic constants of iron at inner-core conditions (Stixrude & Cohen 1995) have shown that the P-wave anisotropy of the HCP phase is identical in symmetry and magnitude to that of the bulk inner core, while that for the FCC phase is considerably greater. Although it is tempting to conclude from these calculations that the observed anisotropy in the core must, therefore, be caused by HCP-Fe, these results do not preclude the presence of an FCC phase, since a polycrystalline aggregate or alloying phase would reduce the inherent anisotropy. Although these calculations were a significant step forward in our understanding of inner-core anisotropy, there is a discrepancy between the calculated elastic constants and those inferred from the latest high-pressure experiments on HCP-Fe (Steinle-Neumann *et al*. 1998), which are considerably higher. Moreover, recent seismic studies have suggested that inner-core anisotropy may be an artefact arising from deep-mantle seismological structure (Creager 1998), or that the inner core itself has some transitional structure between an isotropic upper inner core and an anisotropic lower inner core (Helmberger *et al*. 1998). It is evident that considerable work needs to be done if this problem is to be resolved in the future.

(iii) *Iron alloys in the core*

The composition of the outer core determines both the temperature at the inner core–outer core boundary, where iron is crystallizing out of the liquid outer core, and the convective behaviour of the outer core, which is responsible for the Earth's magnetic field. From seismological evidence, the inferred density of the Earth's outer core is too low by some 10% for it to be comprised purely of iron. Therefore, a number of lighter alloying elements have been suggested to exist in the outer core, although the exact nature and composition of the alloy is uncertain (see Poirier (1994) for a review). Candidates include oxygen, sulphur, silicon, carbon and hydrogen, although it is likely that any, a combination, or all of these could account for the observed density deficit in the outer core. Knowledge of the thermoelastic properties of these

iron alloys fundamentally underpins models of planetary formation and critically controls evolution, yet data at even modest P/T are scarce both theoretically and experimentally. In order to determine the light element in the core, a number of experimental and simulation studies have recently been reported, but often with conflicting results (see, for example, LeBlanc & Secco 1996; Alfè & Gillan 1998; de Wijs *et al*. 1998; Secco 1995). Care must be taken, however, when making such direct comparisons between experiments on candidate iron alloys at the P/T conditions that can currently be attained in a laboratory (Boehler 1992; LeBlanc & Secco 1996; Okuchi & Takahashi 1998) with simulations that are performed at core conditions (see, for example, Sherman 1995; Alfè & Gillan 1998). One of the challenges that faces us for the future is the reconciliation of computational and experimental studies of iron-alloy systems at extreme pressures and temperatures.

5. Conclusions and outlook

We have reviewed some of the recent exciting developments towards our total understanding of the Earth's deep interior. However, there remain many unsolved problems that need to be resolved if we are to fully understand our planet. For example, although the upper mantle and transition zone are relatively well constrained in composition, geotherm and physico-chemical environment, the water content of the transition zone, which could critically affect the melting and transport properties of upper-mantle minerals, is very poorly constrained. As we extend further into the Earth, compositional profiles become less clear; seismic tomography shows compositional heterogeneities in the lower mantle but the time-scale of their stability is not known and is dependent on the convective nature of the lower mantle. However, the viscosity of the lower mantle is poorly constrained with estimates ranging from 10^{16}–10^{21} Pa s at the top of the lower mantle; if there is a non-convecting boundary layer at the base of the lower mantle, as inferred from the superadiabatic geotherm in that region, this would require a significantly higher viscosity. The nature of this super adiabacity has consequences for the origin of the D$''$ zone, a region of compositional, geothermal and seismic heterogeneity just above the core–mantle boundary. Is this a reaction zone, or a ponding zone for subducting slabs? We are even less sure of the Earth's core; the composition and geotherm at core depths are highly speculative. Core temperatures are uncertain to within a few thousand kelvins and the exact nature of the *ca.* 10% light elements is unknown. The temperature at which the inner core is crystallizing out of the outer core will determine the heat flux into the outer core, which, in turn, will determine the convective regime in the outer core that is responsible for the geomagnetic field. The answers to these, and other questions, are not far away.

It is unlikely that we shall ever be able to directly sample the Earth's deep interior; the future of such high-P/T research will depend on the continuing developments in the laboratory that will allow experimentalists to access increasingly higher pressures and temperatures, in conjunction with the rapid advances of supercomputer power that will enable increasingly complex calculations to be performed. The next millennium will see laboratories with microanalytical *in situ* techniques that will not only be able to reach the simultaneously high pressures and temperatures of the Earth's core, but also the extreme conditions to be found in other planets within our Solar System. Advances in the computing industry will enable scientists to have desktop

multi-processor supercomputers that will enable *ab initio* molecular-dynamics simulations on increasingly complex structures to become routine, modelling the properties and processes of planetary materials that critically underpin the formation and evolution of our Solar System.

References

Ahrens, T. J. 1980 Dynamic compression of Earth materials. *Science* **207**, 1035–1041.

Alfè, D. & Gillan, M. J. 1998 First principles simulations of liquid Fe–S under Earth's core conditions. *Phys. Rev.* B **58**, 8248–8256.

Allen, M. P. & Tildesley, D. J. 1987 *Computer simulation of liquids*. Oxford: Clarendon.

Anderson, O. L. & Duba, A. 1997 Experimental melting curve of iron revisited. *J. Geophys. Res.* **102**, 22 659–22 669.

Andrault, D., Fiquet, G., Kunz, M., Visocekas, F. & Häusermann, D. 1997 The orthorhombic structure of iron: an *in situ* study at high temperature and high pressure. *Science* **278**, 831–834.

Bassett, W. A. & Weathers, M. S. 1990 Stability of the body-centred cubic phase of iron – a thermodynamic analysis. *J. Geophys. Res.* **95**, 21 709–21 711.

Boehler, R. 1992 Melting of the Fe–FeO and Fe–FeS systems at high pressure: constraints on core temperatures. *Earth Planet. Sci. Lett.* **111**, 217–227.

Boehler, R. 1993 Temperature in the Earth's core from the melting point measurements of iron at high static pressures. *Nature* **363**, 534–536.

Car, R. & Parrinello, M. 1985 Unified approach for molecular dynamics and density functional theory. *Phys. Rev. Lett.* **55**, 2471–2474.

Catledge, S. A., Vohra, Y. K., Weir, S. T. & Akella, J. 1997 Homoepitaxial diamond films on diamond anvils with metallic probes: the diamond/metal interface up to 74 GPa. *J. Phys. Condens. Matter.* **9**, L67–L73.

Chakraborty, S., Knoche, R., Schultze, H., Rubie, D. C., Dobson, D. P., Ross, N. L. & Angel, R. J. 1999 Enhancement of cation diffusion rates across the 410 km discontinuity in the Earth's mantle. *Science* **883**, 259–262.

Christensen, U. R. 1996 The influence of trench migration on slab penetration into the lower mantle. *Earth Planet. Sci. Lett.* **140**, 27–39.

Cochran, W. 1973 *The dynamics of atoms in crystals*. London: Edward Arnold.

Creager, K. C. 1998 Lateral variations in inner core anisotropy. *AGU Fall Meeting Abstracts* **79**, U42C-05.

Da Silva, C. R. S., Wentzcovitch, R. M., Patel, A., Price, G. D. & Krato, S. I. 1999 The composition and geotherm of the lower mantle: constraints from the calculated elasticity of silicate perovskite. *Phys. Earth Planet. Int.* (Submitted.)

de Wijs, G. A., Kresse, G., Vočadlo, L., Dobson, D., Alfè, D., Gillan, M. J. & Price, G. D. 1998 The viscosity of liquid iron at the physical conditions of the Earths core. *Nature* **392**, 805–807.

Dobson, D. P. & Brodholt, J. P. 1999 The electrical conductivity and thermal structure of the Earth's mid-mantle. *Geophys. Res. Lett.* (Submitted.)

Dobson, D. P., Jones, A. P., Rabe, R., Kato, T., Kondo, T., Kurita, K., Sekine, T., Shimomura, O., Taniguchi, T. & Urakawa, S. 1996 *In-situ* measurement of viscosity and density of carbonate melts at high pressure. *Earth Planet. Sci. Lett.* **143**, 207–215.

Dobson, D. P., Richmond, N. C. & Brodholt, J. P. 1997 A high-temperature electrical conduction mechanism in the lower mantle phase $(Mg,Fe)_{1-x}O$. *Science* **275**, 1779–1781.

Dziewonski, A. M. & Anderson, D. L. 1981 Preliminary reference Earth model. *Phys. Earth Planet. Int.* **25**, 297–356.

Glatzmaier, G. A. & Schubert, G. 1993. Three-dimensional models of layered and whole mantle convection. *J. Geophys. Res.* **98**, 21 969–21 976.

Goarant, F., Guyot, F., Peyronneau, J. & Poirier, J. P. 1992 High-pressure and high-temperature reactions between silicates and liquid iron alloys, in the diamond anvil cell, studied by analytical electron microscopy. *J. Geophys. Res.* **97**, 4477–4487.

Helmberger, D. V., Song, X. & Ni, S. 1998 Seismological evidence for an inner core transition zone. *AGU Fall Meeting Abstracts* **79**, U42C-04.

Hohenberg, P. & Kohn, W. 1964 Inhomogeneous electron gas. *Phys. Rev.* **136**, B864–B871.

Holloway, J. R. & Wood, B. J. 1988 *Simulating the Earth: experimental geochemistry.* Boston, MA: Unwin Hyman.

Irifune, T., Nishiyama, N., Kuroda, K., Inoue, T., Isshiki, M., Utsumi, W., Funakoshi, K., Urakawa, S., Uchida, T., Katsura, T. & Ohtaka, O. 1998 The post-spinel phase boundary in Mg_2SiO_4 determined by *in situ* X-ray diffraction. *Science* **279**, 1698–1700.

Jeanloz, R. & Williams, Q. 1998 The core mantle boundary region. In *Ultrahigh-pressure mineralogy: physics and chemistry of the Earth's deep interior* (ed. R. J. Hemley), pp. 241–259. Washington, DC: MSA.

Kanzaki, M., Kurita, K., Fujii, T., Kato, T., Shimomura, O. & Akimoto, S. 1987 A new technique to measure the viscosity and density of silicate melts at high pressure. In *High pressure research in mineral physics* (ed. M. H. Manghani & Y. Syono), pp. 195–200. Tokyo: Terrapub.

Karato, S.-I., Zhang, S. & Wenk, H. R. 1995 Superplasticity in the Earth's lower mantle: evidence from seismic anisotropy and rock physics. *Science* **270**, 458–461.

Katayama, Y., Tsuji, Y., Chen, J.-Q., Koyama, N., Kikegawa, T., Yaoita, K. & Shimomura, O. 1993 Density of liquid tellurium under high-pressure. *J. Non-Cryst. Solids* **687**, 156–158.

Katsura, T., Sato, K. & Ito, E. 1998 Electrical conductivity of silicate perovskite under lower mantle conditions. *Nature* **395**, 493–495.

Kendall, J. M. & Silver, P. G. 1998 Investigating causes of D″ anisotropy. In *The core–mantle boundary region* (ed. M. Gurnis, M. E. Wysession, E. Knittle & B. A. Buffett), pp. 97–118. Washington, DC: AGU.

Knittle, E. & Jeanloz, R. 1989 Simulating the core–mantle boundary: an experimental study of high-pressure relations between silicates and liquid iron. *Geophys. Res. Lett.* **16**, 609–612.

LeBlanc, G. E. & Secco, R. A. 1996 Viscosity of an Fe–S liquid up to 1300 °C and 5 GPa. *Geophys. Res. Lett.* **23**, 213–216.

Li, X. Y. & Jeanloz, R. 1991 Effect of iron content on the electrical-conductivity of perovskite and magnesiowüstite assemblages at lower mantle conditions. *J. Geophys. Res.* **96**, 6113–6120.

Liu, J. & Vohra, Y. K. 1996 Fluorescence emission from high purity synthetic diamond anvil to 370 GPa. *App. Phys. Lett.* **68**, 2049–2051.

Loper, D. E. & Lay, T. 1995 The core–mantle boundary region. *J. Geophys. Res.* **100**, 6397–6420.

McCammon, C. 1997 Perovskite as a possible sink for ferric iron in the lower mantle. *Nature* **387**, 694–696.

Manga, M. & Jeanloz, R. 1998 Temperature distribution in a laser-heated diamond cell. In *Properties of earth and planetary materials at high pressure and temperature* (ed. M. H. Manghani & T. Yagi), pp. 17–26. Washington, DC: AGU.

Manghani, M. H., Vijayakumar, V. & Bass, J. D. 1998 High-pressure Raman scattering study of majorite-garnet solid solutions. In *Properties of earth and planetary materials at high pressure and temperature* (ed. M. H. Manghani & T. Yagi), pp. 129–138. Washington, DC: AGU.

Mao, H. K & Bell, P. M. 1975 Design of a diamond-windowed, high-pressure cell for hydrostatic pressures in the range 1 bar to 0.5 Mbar. *Carnegie Inst. Washington Yearbook* **74**, 402–405.

Mao, H. K. & Hemley, R. J. 1998 New windows on the Earth's deep interior. *Rev. Mineralogy* **37**, 1–28.

Mao, H. K., Wu, Y., Hemley, J., Chen, L. C., Shu, J. F. & Finger, L. W. 1989 X-ray-diffraction to 302 gigapascals—high-pressure crystal-structure of cesium iodide. *Science* **246**, 649–651.

Martinez, I., Wang, Y. B., Guyot, F., Liebermann, R. C. & Doukhan, J. C. 1997 Microstructures and iron partitioning in (Mg,Fe)SiO_3 perovskite (Mg,Fe)O magnesiowustite assemblages: an analytical transmission electron microscopy study. *J. Geophys. Res.* **102**, 5265–5280.

Matsui, M. 1993 Molecular dynamics study of iron at Earth's inner core conditions. In *AIP Conf. Proc.*, pp. 887–891. American Institute of Physics.

Nguyen, J. H. & Holmes, N. C. 1998 Iron sound velocities in shock wave experiments up to 400 GPa. *AGU Abstracts* **79**, T21D-06.

Okuchi, T. & Takahashi, E. 1998 Hydrogen in molten iron at high pressure: the first measurement. In *Properties of Earth and planetary materials at high pressure and temperature*. AGU Monograph, no. 101, pp. 249–260.

Omura, K. 1991 Change in the electrical conductivity of olivine associated with the olivine–spinel transition. *Phys. Earth. Planet. Int.* **65**, 292–307.

Parker, R. L. 1970 The inverse problem of electromagnetic induction. *Geophys. J. R. Astron. Soc.* **22**, 121–138.

Pasternak, M. P., Taylor, R. D., Jeanloz, R., Li, X., Nguyen, J. H. & McCammon, C. A. 1997 High pressure collapse of magnetism in $Fe_{0.94}O$: Mössbauer spectroscopy beyond 100 GPa. *Phys. Rev. Lett.* **79**, 5046–5049.

Peltier, W. R. & Solheim, L. P. 1992. Mantle phase transitions and layered chaotic convection. *Geophys. Res. Lett.* **19**, 321–324.

Poirier, J. P. 1994 Light elements in the Earth's outer core: a critical review. *Phys. Earth Planet. Int.* **85**, 319–337.

Poirier, J. P., Malavergne, V. & Le Mouël, J. L. 1998 Is there a thin electrically conducting layer at the base of the mantle? In *The core–mantle boundary region* (ed. M. Gurnis, M. E. Wysession, E. Knittle & B. A. Buffett), pp. 131–138. Washington, DC: AGU.

Richmond, N. C. & Brodholt, J. P. 1998 Calculated role of aluminum in the incorporation of ferric iron into magnesium silicate perovskite. *Am. Min.* **83**, 947–951.

Saxena, S. K., Dubrovinsky, L. S. & Häggkvist, P. 1996 X-ray evidence for the new phase of β-iron at high temperature and high pressure. *Geophys. Res. Lett.* **23**, 2441–2444.

Secco, R. A. 1995 In *Mineral physics and crystallography: a handbook of physical constants* (ed. T. J. Ahrens), p. 218. Washington, DC: AGU.

Shankland, T. J., Peyronneau, J. & Poirier, J.-P. 1993 Electrical conductivity of the Earth's lower mantle. *Nature* **366**, 453–455.

Shen, A. H., Reichmann, H.-J., Chen, C., Angel, R. J., Bassett, W. A. & Spetzler, H. 1998*a* GHz ultrasonic interferometry in a diamond anvil cell: P-wave velocities in periclase to 4.4 GPa and 207 °C. In *Properties of Earth and planetary materials at high pressure and temperature* (ed. M. Manghani & T. Yagi), pp. 71–78. Washington, DC: AGU.

Shen, G. Y., Mao, H. K., Hemley, R. J., Duffy, T. S. & Rivers, M. L. 1998*b* Melting and crystal structure of iron at high pressures and temperatures. *Geophys. Res. Lett.* **25**, 373–376.

Sherman, D. M. 1995 Stability of possible Fe–FeS and Fe–FeO alloy phases at high pressure and the composition of the Earth's core. *Earth Plan. Sci. Lett.* **132**, 87–98.

Singh, D. J. 1994 *Planewaves, pseudopotentials and the LAPW method*. Kluwer.

Steinle-Neumann, G., Stixrude, L. & Cohen, R. E. 1998 First principles elastic constants for the HCP transition metals Fe, Co and Re at high pressure. *Phys. Rev.* B **60**, 791–799.

Stixrude, L. 1998 Elastic constraints and anisotropy of $MgSiO_3$ perovskite, periclase and SiO_2 at high pressure. In *The core–mantle boundary region* (ed. M. Gurnis, M. E. Wysession, E. Knittle & B. A. Buffett), pp. 83–96. Washington, DC: AGU.

Stixrude, L. & Bukowinski, M. S. T. 1990 Fundamental thermodynamic relations and silicate melting with implications for the constitution of D″. *J. Geophys. Res.* **95**, 19 311–19 325.

Stixrude, L. & Cohen, R. E. 1995 High pressure elasticity of iron and anisotropy of the Earth's inner core. *Science* **267**, 1972–1975.

Vočadlo, L., Patel, A. & Price, G. D. 1995 Molecular dynamics: some recent developments in classical and quantum mechanical simulation of minerals. *Min. Mag.* **59**, 597–605.

Vočadlo, L., de Wijs, G., Kresse, G., Gillan, M. J. & Price, G. D. 1997 First principles calculations on crystalline and liquid iron at Earth's core conditions. In *Solid-state chemistry—new opportunities from computer simulations*. Faraday Discussions, no. 106, pp. 205–217.

Vočadlo, L., Brodholt, J. Alfè, D., Gillan, M. & Price, G. D. 1999 *Ab initio* calculations on the polymorphs of iron at core conditions. *Phys. Earth Planet. Int.* (Submitted.)

Weidner, D. J., Wang, Y., Chen, G., Ando, J. & Vaughn, T. 1998 Rheology measurements at high pressure and temperature. In *Properties of Earth and planetary materials at high pressure and temperature* (ed. M. Manghani & T. Yagi), pp. 473–482. Washington, DC: AGU.

Wood, B. J. & Rubie, D. C. 1996 The effect of alumina on phase transformations at the 660 kilometer discontinuity from Fe–Mg partitioning experiments. *Science* **273**, 1522–1524.

Wysession, M. E. 1996 Imaging cold rocks at the base of the mantle: the fate of slabs? In *Subduction top to bottom* (ed. G. E. Bebout, D. Scholl, S. Kirby & J. Platt), pp. 369–384. AGU Geophysical Monograph, no. 96.

Wysession, M. E., Lay, T., Revenaugh, J., Williams, Q., Garnero, E. J., Jeanloz, R. & Kellogg, J. H. 1998 The D″ discontinuity and its implications. In *The core–mantle boundary region* (ed. M. Gurnis, M. E. Wysession, E. Knittle & B. A. Buffett), pp. 273–298. Washington, DC: AGU.

Xu, Y., Poe, B. T., Shankland, T. J. & Rubie, D. C. 1998*a* Electrical conductivity of olivine, wadsleyite and ringwoodite under upper-mantle conditions. *Science* **280**, 1415–1418.

Xu, Y., McCammon, C. & Poe, B. T. 1998*b* The effect of alumina on the electrical conductivity of silicate perovskite. *Science* **282**, 922–924.

Yagi, T. & Funamori, N. 1996 Chemical composition of the lower mantle inferred from the equation of state of $MgSiO_3$ perovskite. *Phil. Trans. R. Soc. Lond.* A **354**, 1371–1384.

AUTHOR PROFILES

David Dobson

After graduating from Bristol University in 1991 with upper second class honours in geology, David Dobson moved to University College London in 1992 to study for a PhD. David obtained his PhD in 1995, has since has been a postdoctoral research fellow and is currently a NERC fellow, both at UCL. While at Bristol, David was awarded the Donald Ashby Prize and he is the 1999 Geological Society of London's President's Award recipient, at the age of 29. His primary research interests are in high-pressure experimental petrology, while out of the laboratory he is a keen mountaineer and artist.

Lidunka Vočadlo

Lidunka Vočadlo studied at University College London, where she graduated with upper second class honours in Physics and Astronomy in 1988. After gaining a PGCE at the Institute of Education in 1989, she obtained her PhD in 1993 in the Geological Sciences Department at UCL. She has remained in the Geological Sciences Department ever since, doing postdoctoral research from 1993 to 1996 and as a UCL Research Fellow from 1996 to 1999. In 1998, Lidunka was awarded the Dornbos Memorial Prize for young researchers and in 1999, aged 32, she was awarded a Royal Society University Research Fellowship. Her primary research interest lies in the computer simulation of Earth and planetary materials. She relaxes with long sunny days on top of the fells in the Lake District and long cool evenings drinking fine wine, watching them slide into the night.